Applied and Computational Mechanics 7 (2013) 39–52

Influence of delayed excitation on vibrations of turbine blades couple

L. Půst[a,*], L. Pešek[a]

[a]Institute of Thermomechanics ASCR, Dolejškova 5, 182 00 Prague 8, Czech Republic

Received 29 January 2013; received in revised form 6 June 2013

Abstract

In the presented paper, the computational model of the turbine blade couple is investigated with the main attention to the influence two harmonic excitation forces, having the same frequency and amplitude but with moderate delay in time. Time delay between the exciting harmonic forces depends on the revolutions of bladed disk, on the number of blades on a rotating disk and on the number of stator blades. The reduction of resonance vibrations realized by means of dry friction between the shroud blade-heads increases roughly proportional to the difference of stator and rotor blade-numbers and also to the magnitude of dry friction force.

From the analysis of blade couple with direct contact it was proved that the increase of friction forces causes decrease of resonance peaks, but the influence of elastic micro-deformations in the contact surfaces (modeled e.g. by the modified Coulomb dry friction law) is rather small.

Analysis of a blade couple with a friction element shows that the lower number of stator blades has negligible influence on the amplitudes of both blades, but decreases amplitudes of the friction element oscillations. Similarly the increase of friction forces causes a decrease of resonance peaks, but an increase of friction element amplitudes.

Keywords: time delay, phase delay, blades couple, amplitude reduction, dry friction

1. Introduction

The enormous great resonance vibrations of turbine blades are very dangerous and are often the cause of serious crashes of power plants. The reduction of undesirable vibrations of turbine blades is very often realized by using the blade damping heads. A lot of theoretical, numerical and experimental studies were done in the Institute of Thermomechanics ASCR in cooperation with the University of West Bohemia on the problems of ascertaining the dynamic properties of bladed disks and of reduction of undesirable vibrations.

The main experimental set in laboratories of Institute of Thermomechanics ASCR is a model of a turbine disk, with blades connected either by direct contact or by an inserted friction element. There are many articles and books related to theoretical and experimental investigations of friction properties, e.g. [4, 13]. However, the literature sources on friction properties are mainly oriented to the study of friction properties at constant or slowly variable relative velocity in the friction contact surfaces, which is important e.g. for bearings, clutch, brakes, etc., but the friction at vibrations, where the contact velocity varies from positive to negative values in one period, has been given small attention. As an example let us mention book [2], where the friction processes are investigated on the various types of analytical models. Friction at vibrating, particularly stick-slip motion, are solved in [1, 3, 16], mainly for sphere contacts.

*Corresponding author. Tel.: +420 266 053 212, e-mail: pust@it.cas.cz.

The application of friction contact to the damping of blades systems occurs very often in praxis and also in technical literature. The friction properties in blade contact surfaces are analyzed in [5], properties of damper near the blade root are solved in [8] and [12]. The Influence of contact stiffness is considered in [15]. Numerical analysis of shroud friction blades contact by FE method is presented in [14]. No solution of phase-delayed excitation of blade couple with friction contact has been found in any accessible literature.

For detail discovering of friction processes and their influence on blades vibrations, the dynamic tests of separated blade couple connected by [11] describes the influence of various mathematical models of dry friction forces (modified Coulomb [9], spring-dry friction model [6], etc.) on the response curves of harmonically excited blade couple. In paper [7], there it is shown the additional effect of elastic stops, fixed to the friction element in order to prevent falling out of the slot during vibrations, both on reduction of amplitudes, but also on appearance of instability regions and existence of chaotic oscillations.

The dynamic systems investigated in both papers have two or three degrees of freedom, shown in Fig. 1 and were (unlike to here investigated system) excited only by one harmonic force $F_0 \cos \omega t$ acting on the first blade. The right hand subsystem was without any external excitation.

In the present paper, the same blades systems modeled by two or three degrees of freedom mathematical models are investigated with the main attention to the influence of the second excitation force, having the same frequency and amplitude but being moderately delayed in time. Parameters of these mathematical models were determined from the experimental models used in laboratory IT ASCR by means of eigenfrequency measurements and vibration amplitude decay of blade after the abrupt switching of excitation in resonance.

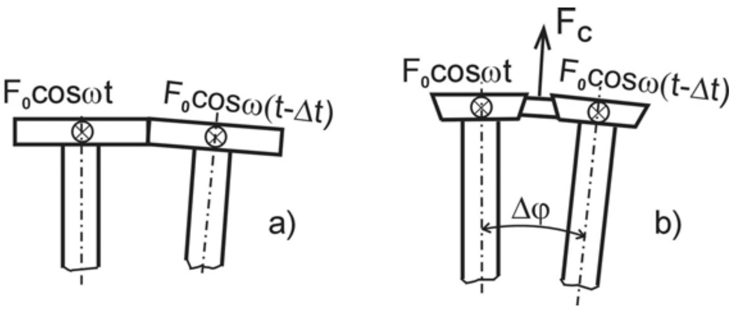

Fig. 1. Friction connection of blades

The reduction of undesirable vibrations of blades is realized by using blade damping heads, which are connected by either a direct friction contact (position a) or by inserted friction elements (position b), as seen in Fig. 1. In the first case, due to the de-twisting of both blades at rotation, the pressure in the appropriate contact surface produces friction losses and in consequence of this also the reduction of vibrations. In alternative b), the head tops of the blades are provided with the friction surfaces creating the wedge-shaped inter-head slot. The friction element is pushed in the slot by the centrifugal force under rotation or for non-rotating stationary tests by the static force F_c.

The blades vibrate in bending and torsion modes. It has been shown in [3], that blades in the real turbines have sufficiently high torsion eigenfrequencies and therefore their mutual interaction with the first bending mode is negligible. In this contribution, only the bending modes will be taken into account.

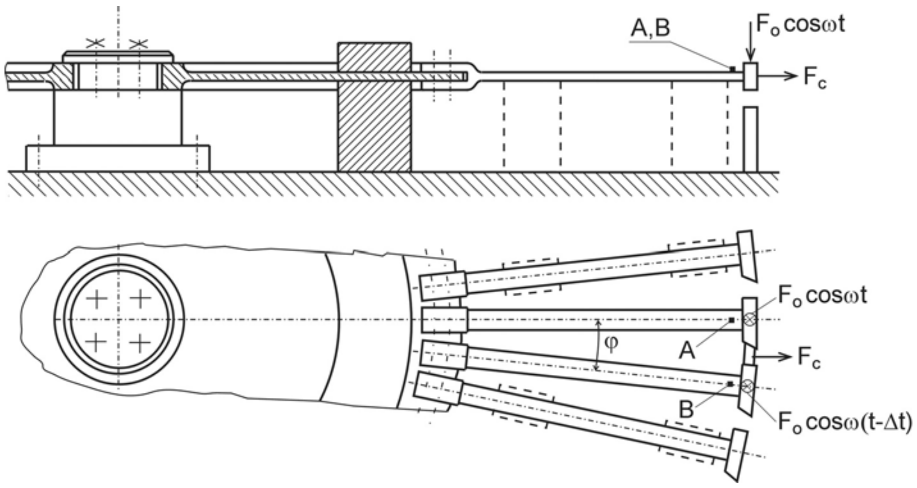

Fig. 2. Measurement of blade couple with inserted friction element

Laboratory measurements of a blade couple were realized on two selected blades, the roots of which were joined to the experimental disk, which was rigidly fastened to a steel plate basement. The other blades, except for the mentioned couple, were fastened to the steel plate as well — see Fig. 2.

2. Delay of excitation

In both cases of the blade-heads connection, the right blade is forced by a delayed harmonic force $F_0 \cos\omega(t - \Delta t)$. The time delay Δt of periodic excitation depends on the revolutions

$$n = \frac{60\omega_r}{2\pi} \tag{1}$$

of the bladed disk, on number l_r of blades on rotating disk and on number l_s of stator blades. Basic frequency f_e of excitation of an individual blade from the periodic distribution of pressure on the outflow behind the stator blade row is

$$f_e = \frac{n}{60} l_s, \qquad \omega_e = 2\pi f_e = \frac{2\pi}{60} n l_s. \tag{2}$$

The next blade is excited by the same excitation frequency f_e, but delayed on the time interval Δt proportional to the angle between l_r blades $\Delta\varphi = 2\pi/l_r$. This time interval is given by

$$\Delta t = \Delta\varphi/\omega_r = \frac{2\pi}{l_r} / \frac{2\pi}{60} n = \frac{60}{l_r n}. \tag{3}$$

The exciting angular frequency at static experiments is $\omega = \omega_e$. Using (1) and (2) gives

$$\Delta t = \frac{60}{l_r n} = \frac{60}{l_r} \cdot \frac{1}{60\omega_e/2\pi l_s} = \frac{2\pi}{\omega} \cdot \frac{l_s}{l_r}. \tag{4}$$

The shifted excitation force acting on the second blade is

$$F_0 \cos\omega(t - \Delta t) = F_0 \cos\omega \left(t - \frac{2\pi}{\omega} \cdot \frac{l_s}{l_r} \right) = F_0 \cos \left(\omega t - 2\pi \cdot \frac{l_s}{l_r} \right), \tag{5}$$

where the delay is in the last formula expressed as phase angle shift, in the middle formula as the time shift.

3. Vibrations of a blade couple with a direct friction contact

A simplified mathematical model of such a couple is shown in Fig. 3. This model consists of two identical 1 DOF slightly damped subsystems connected by a direct friction contact. Blade's bending and damping were modeled by stiffness k and damping coefficient b, roughly corresponding to the experimentally ascertained values. As this analysis is limited to the lowest resonance frequency, the modeling by 1 DOF is eligible.

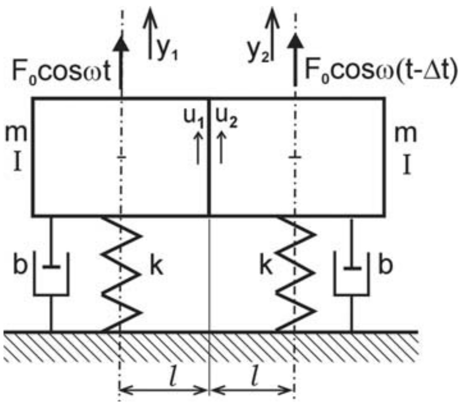

Fig. 3. Mathematical model of two blades system with direct friction contact

The analysis of up to now investigated model of blade couple with friction contact has been solved at the assumption that blades vibrate only in the bending mode. If we neglect a torsion vibration of blades, the velocities $\dot{u}_1$, $\dot{u}_2$ in the friction surfaces are

$$\dot{u}_1 = \dot{y}_1, \qquad \dot{u}_2 = \dot{y}_2. \tag{6}$$

Differential equations of motion are

$$\begin{aligned} m\ddot{y}_1 + b\dot{y}_1 + ky_1 + F_t(\dot{u}_1 - \dot{u}_2) &= F_0 \cos\omega t, \\ m\ddot{y}_2 + b\dot{y}_2 + ky_2 - F_t(\dot{u}_1 - \dot{u}_2) &= F_0 \cos\omega(t - \Delta T), \end{aligned} \tag{7}$$

where $\dot{u}_1 - \dot{u}_2 = \dot{y}_1 - \dot{y}_2$.

After substituting $\dot{u}_1$, $\dot{u}_2$ from (6) into (7) and using (5) we get equations with two unknown quantities y_1, y_2:

$$\begin{aligned} m\ddot{y}_1 + b\dot{y}_1 + ky_1 + F_t(\dot{y}_1 - \dot{y}_2) &= F_0 \cos\omega t, \\ m\ddot{y}_2 + b\dot{y}_2 + ky_2 - F_t(\dot{y}_1 - \dot{y}_2) &= F_0 \cos\left(\omega t - 2\pi \tfrac{l_s}{l_r}\right). \end{aligned} \tag{8}$$

Expression $F_t(\dot{y}_1 - \dot{y}_2) = F_t(\dot{u}_1 - \dot{u}_2)$ describes the dry friction forces in the heads slot.

Differential equations (7), (8) as well as (11) together with additional expressions (9), (10), (12) were solved in MATLAB R2012a version, using Runge-Kutta 4$^{\text{th}}$ order integrating methods. The time steps were $0.000\,1$ s in order to describe the sudden jumps of dry friction forces and other strong nonlinearities with sufficient accuracy. Numerical simulations give time histories of motion $y_1(t), y_2(t), y_3(t)$, from which the maxima of y_i i.e. amplitudes a_i were ascertained and plotted.

4. Dry friction properties

Dry friction is very complicated, strongly nonlinear process and the generally used Coulomb's model is only the first approximation of real properties. For a better description of friction process, the stick-slip (or micro slip-full slip) model is often used. The short survey of basic mathematical models giving at least approximate true pictures of real forces is in [4]. The influence of application of some dry friction model on the blade couple vibration will be presented in the next chapters.

The first improvement of the classical Coulomb friction law

$$\begin{aligned} F_t = F_{t_0}\,\mathrm{sgn}\,(v) \quad & \text{for } |v| > 0, \\ -F_{t_0} < F_t < F_{t_0} \quad & \text{for } v = 0 \end{aligned} \tag{9}$$

is the modified Coulomb law, where instead of the sudden jump at zero velocity at the very low velocity v, the complicated processes caused mostly by elastic micro-deformations of bodies near the friction surfaces, accompanied by partial micro-slip in several points of the contact area, are modeled by a oblique line, a linear increase of friction force, as shown in Fig. 4.

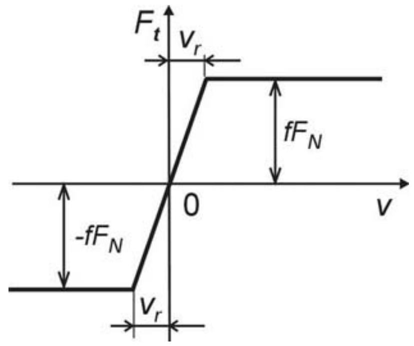

Fig. 4. Modified Coulomb friction characteristics

Micro-slips arise in the contact points, where owing to non-uniform distribution of contact pressure a part of the area is less loaded or even without contact. Processes, which happen during this motion period, are therefore always highly influenced by wear, geometry of contact bodies, precision of surfaces, etc. Their mathematical model is therefore very uncertain and the oblique line is the first approximation of the real micro-deformations and micro-slips processes.

Critical velocity v_r [m/s] is a velocity, at which the micro-slip motion changes into full relative motion, F_{t_0} is Coulomb friction force, proportional to the normal pressure $F_{t_0} = fF_N$ [N]. Mathematical description of the simply modified Coulomb law with the constant dry friction force $F_{t_0} = \pm fF_N$ in the full slip phase of motion is:

$$F_t = F_{t_0}\left[\frac{v}{v_r}H(v_r - |v|) + \mathrm{sgn}\,(v)H(|v| - v_r)\right], \tag{10}$$

where H is the Heaviside function. Normal force F_N [N] acts in the contact surface between the modelled bodies. This force is in the real turbine blading realized by the un-twisting of blades due to the centrifugal force at couples with direct contact, or by indentation of friction element into slot between blades heads, again due to the centrifugal force at rotation.

This basic dry-friction model can be completed by further functions expressing e.g. a simple linear increase or decrease of friction force at higher relative velocities. To express friction force that at great velocity v settles on a constant value, it is possible to use the functions $\mathrm{atan}\,(v)$ or $\exp(-v)$.

5. Example of a system with direct friction contact

Applying equations (4) for parameters roughly corresponding to the experimental set, i.e. $m = 0.2\,\mathrm{kg}$, $k = 100\,000\,\mathrm{N/m}$, $F_0 = 1\,\mathrm{N}$, $F_1(t) = F_0 \cos \omega t$, $F_2(t) = F_0 \cos \omega(t - \Delta t)$, the amplitude response curves of all three coordinates y_1, y_2, $u_1 - u_2$ can be calculated for several cases of time delay (i.e. different number l_s, l_r of stator and rotor blades), friction forces, types of friction characteristics and damping coefficients of the separate blades.

The acceleration of sweeping excitation frequency ω at simulation is sufficiently low

$$\frac{\mathrm{d}\omega}{\mathrm{d}t} = accel = 0.25\ \mathrm{rad/s^2}$$

so that the transient response is very close to the stationary one. It can be proved by recording response curves of mathematical model with increasing and decreasing excitation frequency — as shown in Fig. 5 for the twofold passing acceleration $0.5\ \mathrm{rad/s^2}$ and for the system with inserted friction element. Damping of both blades is modeled by small viscous damping with coefficients $b_1 = b_2 = 0.1$ Ns/m.

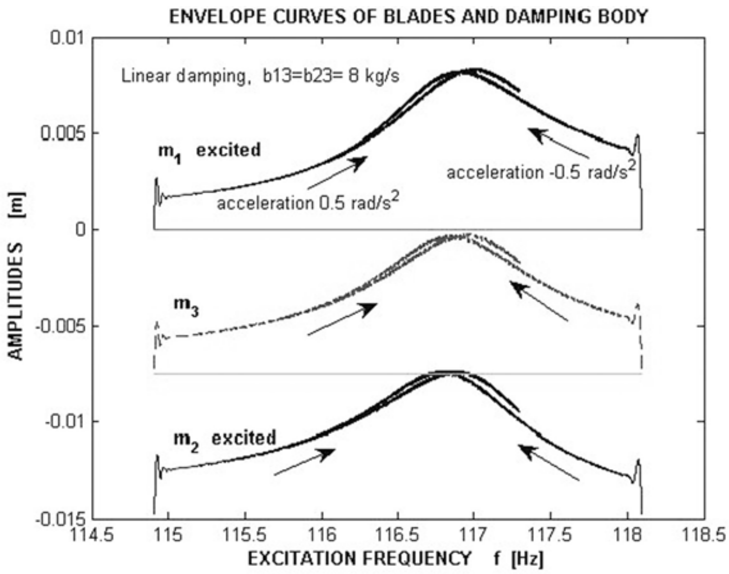

Fig. 5. Check of distortion at sweep excitation

The shifts of peaks is $df = 0.03$ Hz, which related to the resonance frequency gives error smaller than 0.03 %.

6. Phase-shift effect on a system with direct Coulomb friction contact

If there is no phase shift between fully synchronized exciting forces, no relative motion in the contact surface exists and the system is damped only by the small subsystem's damping forces $b\dot{y}_i$, $i = 1, 2$. Resonance amplitudes in such a case are very high (the frequency range in the figures is only 1.5 Hz). However due to delay of one harmonic exciting force against the other, relative motion connected with the friction energy losses in the contact surface occurs and resonance amplitudes get lower. For the equal subsystems with masses $m = 0.2$ kg and spring stiffness $k = 100\,000\ \mathrm{kg \cdot s^{-2}}$, the amplitude response curves $a_1(f)$, $a_2(f)$ are drawn in Fig. 6 for dry friction force $F_t = 0.2$ N and for six blade-number ratios

$$l_s/l_r = 1; 0.9; 0.8; 0.7; 0.6; 0.5.$$

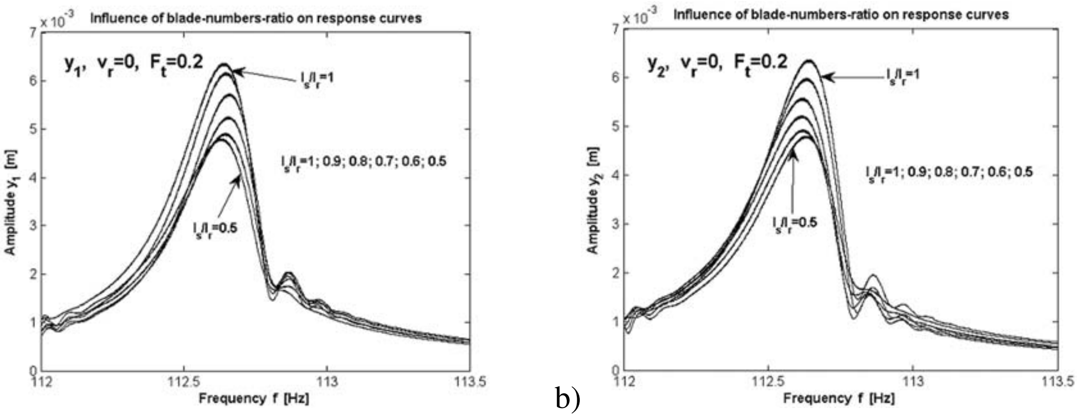

a) b)

Fig. 6. Influence of excitation delay at dry friction force $F_T = 0.2$

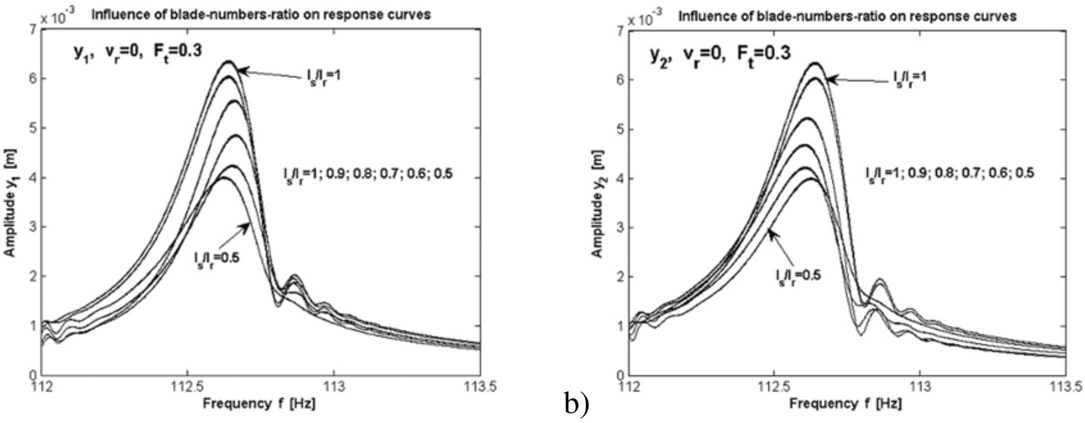

a) b)

Fig. 7. Influence of excitation delay at dry friction force $F_T = 0.3$

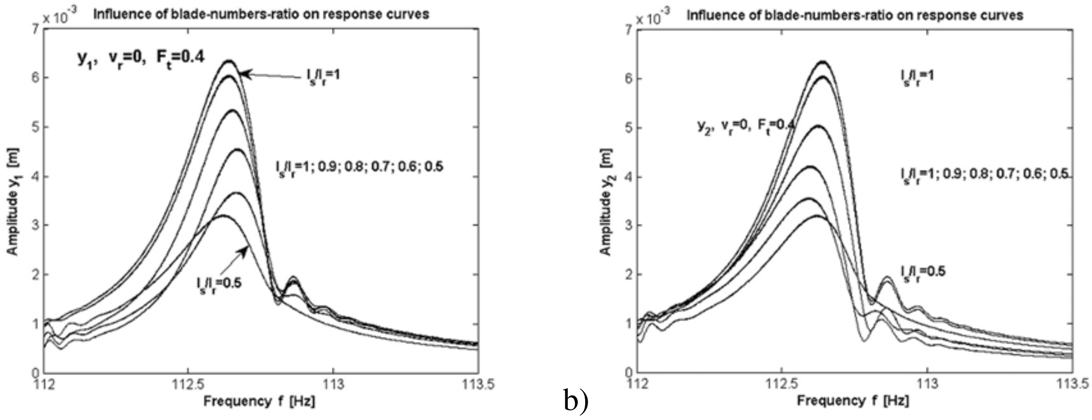

a) b)

Fig. 8. Influence of excitation delay at dry friction force $F_T = 0.4$

Similar curves are plotted in Fig. 7 for the higher dry friction force $F_t = 0.3$ N and again for six blade-number ratios. Influence of the dry friction force $F_t = 0.4$ N is shown in Fig. 8. It is evident that the damping increases with higher friction force and with greater difference between the number l_s of stator blades and number l_r of rotor blades.

The elastic micro-deformations in contact surfaces (as well as small torsion deformations- in this analysis neglected) can reduce the positive dry friction damping effect. It can be shown on the case where a modified Coulomb dry friction model (see Fig. 4) is used.

7. Phase-shift effect — modified Coulomb dry friction

The influence of elastic micro-deformations in the contact surfaces can be analyzed by using various more sophisticated mathematical models. The simplest one is the modified Coulomb dry friction model containing two parameters: critical velocity v_r at which the partial micro-slip motion changes into full slip motion and vice versa and the constant friction force $F_{t_0} = \pm f F_N$ in the full slip at higher velocities.

Because the maximum amplitude is the decisive value for the reliability of blades systems, the influence of phase-shift excitation and critical velocity v_r on the high of resonance amplitude will be considered.

Response curves for four values of critical velocity $v_r = 0, 2, 4, 6$ and for ratio of the number of stator and rotor blades $l_s/l_r = 0.7$ are shown in Fig. 9. The greater is the critical velocity, the smaller is the damping ability of friction connection. Interesting phenomenon is the increase of first blade's amplitudes in the under-resonance zone and the increase of the second blade's amplitudes in the over-resonance zone.

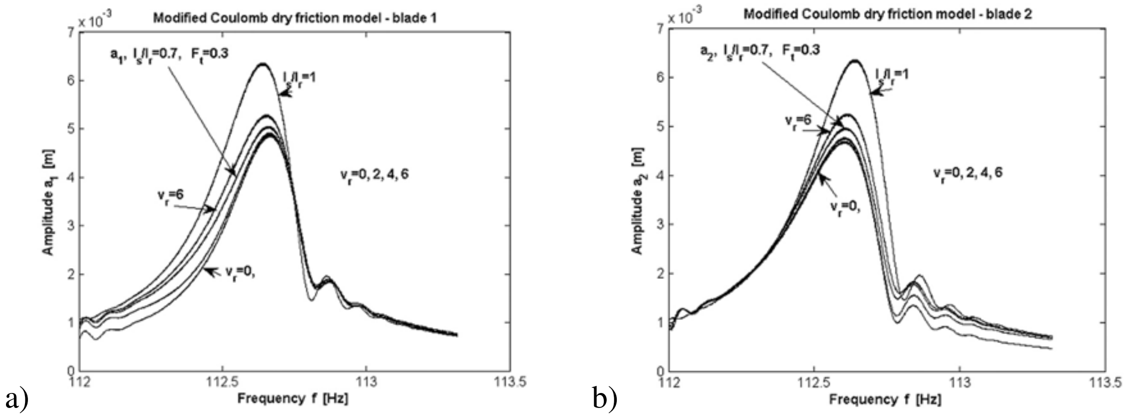

Fig. 9. Influence of critical velocity v_r at $F_T = 0.3$ and at ratio $l_s/l_r = 0.7$

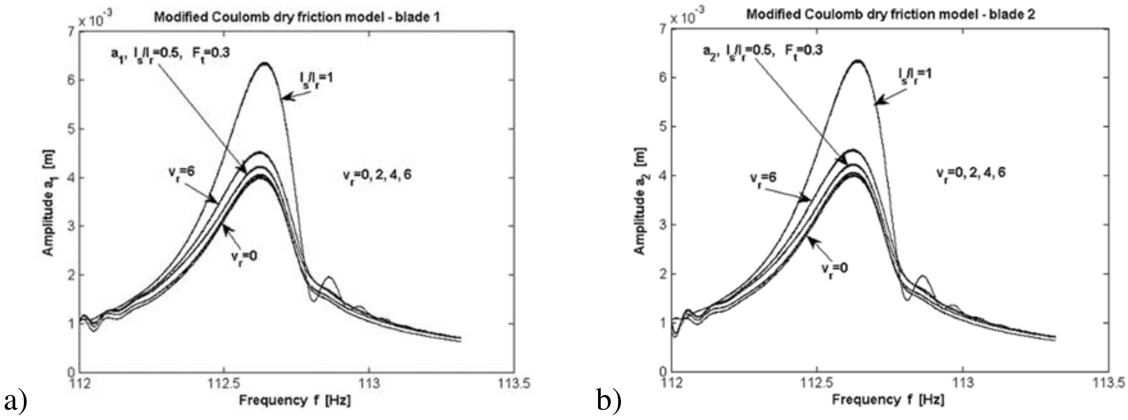

Fig. 10. Influence of critical velocity v_r at $F_T = 0.3$ and at ratio $l_s/l_r = 0.5$

In order to estimate the damping contribution caused by the phase-shift excitation, one response curve at in phase excitation $l_s/l_r = 1$ is plotted in each diagram.

For the same system parameters but for smaller ratio of the numbers of stator and rotor blades $l_s/l_r = 0.5$, the response curves again for four values of critical velocity $v_r = 0, 2, 4, 6$ are shown in Fig. 10. The quenching of amplitudes is now greater than in the previous case and the damping ability of friction connection decreases again with growing critical velocity.

Interesting phenomenon in this case is the identity of both sets of amplitude response curves $a_1(f)$ and $a_2(f)$ (the phase response curves are however different), as well as the increase of amplitudes both in the before-resonance and in the after-resonance zone with the increasing of critical velocity v_r.

8. Vibrations of a blade couple with friction element

Experimental research gives important results useful for design and development of new machines, but it is e.g. difficult to measure motion of friction element, dry friction forces and friction coefficient during operation, etc.

Therefore the additional analytical and numerical solution of simplified mathematical model with exact parameters is very useful and enables to complete knowledge of dynamic behavior of studied system with new information. Experimental system in Fig. 1 can be modeled by a simple three masses system shown in Fig. 11, where the blades are replaced by 1 DOF systems.

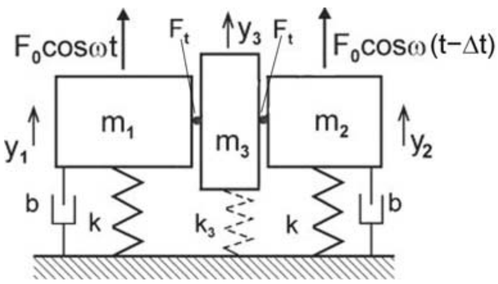

Fig. 11. Mathematical model of two blades system with friction element

Damping of both blades is in Fig. 11 modeled by small viscous damping with coefficients $b_1 = b_2 = 0.1$ Ns/m. For elimination of gravitational force, the friction element $m_3 = 0.02$ kg was supported by a very weak spring with stiffness $k_3 = 100$ N/m. Differential equations of motion are then

$$\begin{aligned} m_1\ddot{y}_1 + b_1\dot{y}_1 + k_1y_1 + g_1(\dot{y}_1 - \dot{y}_3) &= F_0\cos\omega t, \\ m_2\ddot{y}_2 + b_2\dot{y}_2 + k_2y_2 + g_2(\dot{y}_2 - \dot{y}_3) &= F_0\cos\omega(t - \Delta t), \\ m_3\ddot{y}_3 + k_1y_3 + g_1(\dot{y}_1 - \dot{y}_3) - g_2(\dot{y}_2 - \dot{y}_3) &= 0, \end{aligned} \tag{11}$$

where the excitation frequency of force $F_0\cos\omega t$ varies near to the eigenfrequencies of main subsystems

$$\omega \approx \sqrt{k_1/m_1} \approx \sqrt{k_2/m_2}.$$

The nonlinear functions g_1, g_2 consist of nonlinear Coulomb dry friction damping forces:

$$g_i = F_{ti}\,\mathrm{sgn}\,(\dot{y}_i - \dot{y}_3), \qquad i = 1, 2, \tag{12}$$

where H is the Heaviside function.

Motion of the investigated system is further solved by direct numerical solution of equations (11), (12).

9. Example of a blade couple with friction element

Only the dry frictions connect the three masses system. Amplitude response curves $a_1(f)$, $a_2(f)$, $a_3(f)$ of systems with four different delays given by blades' numbers $l_s/l_r = 1; 0.8; 0.6; 0.5$ are calculated and drawn in Fig. 12a–c for the equal main subsystems parameters: $m_1 = m_2 = 0.2\,\mathrm{kg}$, $k = 100\,000\,\mathrm{kg\cdot s^{-2}}$, $m_3 = 0.02\,\mathrm{kg}$, dry friction damping force $F_t = 0.3\,\mathrm{N}$ and for stiffness of supporting spring $k_3 = 100$ N/m. Response curves $a_1(f)$ of mass m_1 are almost identical with the response curves $a_2(f)$ of mass m_2 and their forms are also unchanged for various delays $l_s/l_r = 1; 0.8; 0.6; 0.5$, as can be seen from the records in Fig. 12a,b, where the drawings of individual curves are vertically shifted for easy comparison. On the contrary, the amplitudes a_3 of the friction element m_3 are strongly influenced by the change of delays between excitation forces, as it is evident from the records in Fig. 12c for various ratios l_s/l_r. Motion a_3 of friction element m_3 contains chaotic components, which are also contained, however in a smaller rate, in motions a_1, a_2 of the much greater masses m_1 and m_2.

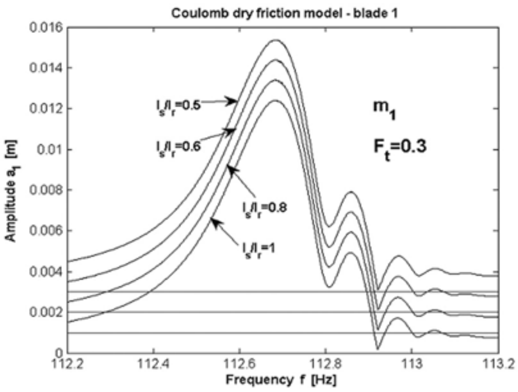

a)

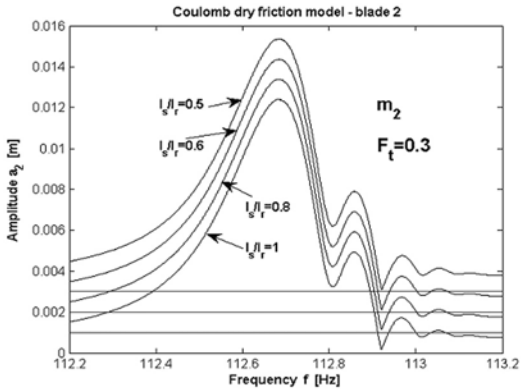

b)

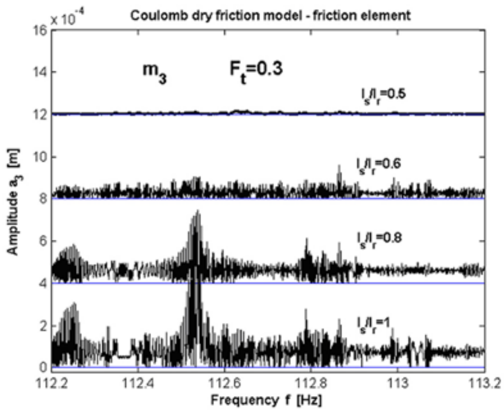

c)

Fig. 12. Influence of different blades ratio $l_s/l_r = 0.5$; 0.6; 0.8; 1 at $F_T = 0.3$

Influence of dry friction forces F_t (Coulomb friction, equation (9)) on the response curves is represented in Fig. 13a–c. Response curves $a_1(f)$ of mass m_1 are again identical with the response curves $a_2(f)$ of mass m_2, but the increase of friction force F_t very strongly decreases the maximum resonance amplitudes, as can be seen from the records in Fig. 13a,b.

Response curves of the amplitudes a_3 of the friction element m_3 are very flat without any resonance peaks. Amplitude a_3 has — at given F_0 — constant value in the majority of frequency range. With increasing friction force F_t, the mean value of amplitude a_3 increases, as it is

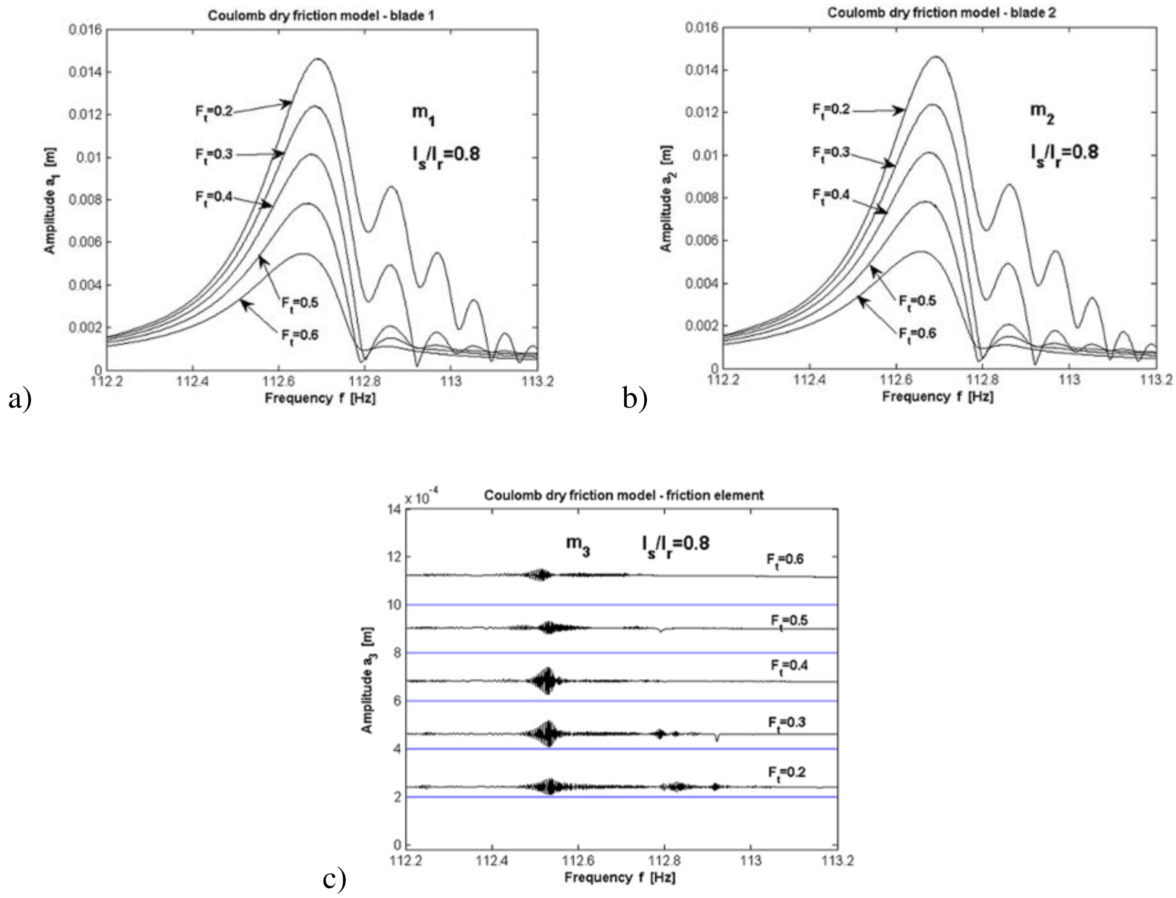

Fig. 13. Influence of different dry friction forces $F_T = 0.2$–0.6 at $l_s/l_r = 0.8$

evident from the records in Fig. 13c for various friction forces. Motion a_3 of friction element m_3 contains, except a constant value, also some oscillating components, but only in narrow frequency ranges near to the rising parts of $a_1(f)$, $a_2(f)$ response curves.

Another properties were obtained, when instead of classical Coulomb friction law (9), the modified Coulomb friction law (10) has been used. Influence of variation of critical velocity v_r on the amplitude response curves $a_1(f)$, $a_2(f)$, $a_3(f)$ of systems with five different critical velocities $v_r = 0, 0.2, 0.4, 0.6, 0.8$ m/s is presented in Fig. 14. Dry friction force $F_t = 0.8$ N is for all response curves constant, as well as the constant excitation delay characterized by the ratio blades' numbers $l_s/l_r = 0.8$. From the diagrams plotted in Fig. 14a,b it is evident that the increase of critical velocity v_r causes moderate increase of resonance peaks of both masses, but as it is shown in Fig. 14c, it causes qualitative change of friction element motion. At $v_r = 0$ (Coulomb friction), the sudden jump of friction force excites irregular, chaotic motion, but at $v_r > 0$ (modified Coulomb friction), the smooth passage between opposite friction forces makes the oscillation of friction element harmonic with smoothly variable amplitudes.

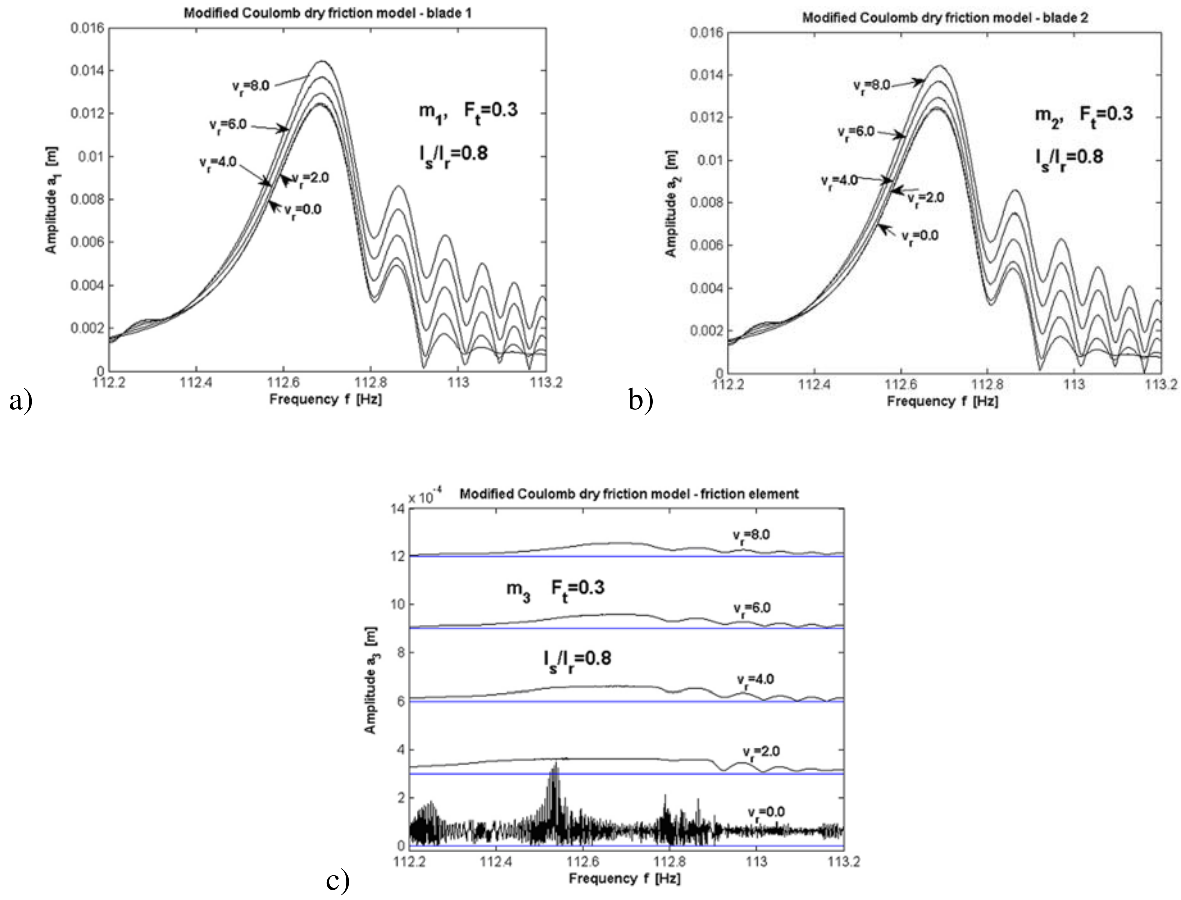

Fig. 14. Influence of different critical velocity v_r at $F_T = 0.3$ and at ratio $l_s/l_r = 0.8$

10. Conclusion

- Present paper serves as further contribution to the systematic research of dynamic properties of turbine blade couple. The introduction of excitation with delay into a mathematical model brings this model closer to a real situation in a working turbine.
- Phase shift of excitation can be expressed either by time delay or by phase (angle) delay.
- This delay is ascertained both by the revolution and by the ratio of numbers of stator and rotor blades.

Blade couple with direct contact:

- The damping ability of blade heads with direct friction contact increases with the lower number of stator blades.
- The increase of friction forces causes a decrease of resonance peaks.
- The elastic micro-deformations in contact surfaces (modelled e.g. by the modified Coulomb dry friction law) decrease the damping ability, but this influence is rather small.

Blade couple with friction element:

- The lower number of stator blades (increasing delay) has a negligible influence on the amplitudes of both blades, but decreases amplitudes of friction element oscillations.
- The increase of friction forces causes decrease of resonance peaks, but an increase of friction element amplitudes.
- Increase of critical velocity v_r causes moderate increase of resonance peaks of both masses and a qualitative change of friction element motion.

Note: This contribution is an extended text of paper [10].

Acknowledgements

This work has been elaborated in a frame of the grant project GA CR101/09/1166 "Research of dynamic behavior and optimization of complex rotating system with non-linear couplings and high damping materials" and it is also a contribution to the scientific cooperation with NAS Ukraine.

References

[1] Archard, J. F., Contact and rubbing of flat surfaces, Journal of Applied Physics 24 (8) (1953) 981-988.

[2] Awrejcewicz, J., Pyryev, Yu., Nonsmooth dynamics of contacting thermoelastic bodies, Springer, 2009.

[3] Gallego, L., Nelias, D., Modeling of fretting wear under gross slip and partial slip conditions, Journal of Tribology 129 (3) (2007) 528-536.

[4] Guran, A. (ed.), Impact and friction of solids, structures and intelligent machines, World Scientific, Singapore, Series B, Vol. 14, 2000.

[5] Koh, K.-H., Griffin, J. H., Filippi, S., Akay, A., Characterization of turbine blade friction dampers, Journal of Engineering for Gas Turbines and Power-transactions of The ASME 127 (4) (2005) 856-862.

[6] Pešek, L., Půst, L., Influence of dry friction damping on bladed disk vibration. In: Vibration Problems ICOVP 2011, Berlin, Springer, 2011, pp. 557-564.

[7] Pešek, L., Půst, L., Mathematical model of a blade couple connected by damping element, Proceedings of the 8th International Conference on Structural Dynamics, EURODYN 2011, Leuven, Katolieke Universiteit Leuven, 2011, pp. 2 006-2 011.

[8] Pfeifer, F., Hajek, M., Stick-slip motion of turbine blade dampers, Philosophical Transactions of the Royal Society A-Mathematical, Physical and Engineering Sciences 338 (1651) (1992) 503-517.

[9] Půst, L., Pešek, L., Friction in blade system, Proceedings of the conference Computational Mechanics 2011, Pilsen, Book of abstracts, CD ROM edition, 2011.

[10] Půst, L., Pešek, L., Phase delayed excitation of turbine blades couple with friction connection, Proceedings of the conference Computational Mechanics 2012, Špičák, Book of extended abstracts, CD ROM edition, 2012.

[11] Půst, L., Pešek, L., Various types of dry friction characteristics, Proceedings of the conference Dynamika strojů 2011, Prague, Institute of Thermomechanics AS CR, 2011, pp. 77-78. (in Czech)

[12] Rao, J. S., et al., Interface damping in attachment region, Proceedings of the 3rd International Conference on Rotordynamics, IFToMM, CNRS, Lyon, 1990, pp. 185-190.

[13] Sextro, W., Dynamical contact problems with friction, Springer-Verlag, Berlin Heidelberg, 2007.

[14] Szwedowicz, J., The reliable numerical analysis of shrouded bladed disk, In: International Contact Mechanics Workshop, New Orleans, 2001, pp. 1-6.

[15] Voldřich, J., Morávka, Š., Contact stiffness modeling in numerical analysis of nonlinear vibrations of bladed disk with friction contact interfaces, Proceedings of the conference Vibration Problems ICOVP 2011 — Supplement, TU Liberec, 2011, pp. 383-388.

[16] Yang, B. D., Chu, M. L., Meng, C. H., Stick-slip-separation analysis and non-linear stiffness and damping characterization of friction contacts having variable normal force, Journal of Sound and Vibration 210 (4) (1998) 461-481.